The Astronomical Journal, 147:129 (11pp), 2014 June doi:10.1088/0004-6256/147/6/129

THE WHITE DWARFS WITHIN 25 pc OF THE SUN: KINEMATICS AND SPECTROSCOPIC SUBTYPES

Edward M. Sion[1], J. B. Holberg[2], Terry D. Oswalt[3], George P. McCook[1], Richard Wasatonic[1], and Janine Myszka[1]
[1] Department of Astronomy & Astrophysics, Villanova University, Villanova, PA 19085, USA;
edward.sion@villanova.edu, george.mccook@villanova.edu, richard.wasatonic@villanova.edu, janine.myszka@villanova.edu
[2] Lunar and Planetary Laboratory, University of Arizona, Tucson, AZ 75201, USA; holberg@vega.lpl.arizona.edu
[3] Department of Physics and Space Sciences, Florida Institute of Technology, Melbourne, FL 19085, USA; toswalt@fit.edu
Received 2013 July 5; accepted 2014 January 17; published 2014 May 1

ABSTRACT

We present the fractional distribution of spectroscopic subtypes, range and distribution of surface temperatures, and kinematical properties of the white dwarfs (WDs) within 25 pc of the Sun. There is no convincing evidence of halo WDs in the total 25 pc sample of 224 WDs. There is also little to suggest the presence of genuine thick disk subcomponent members within 25 pc. It appears that the entire 25 pc sample likely belongs to the thin disk. We also find no significant kinematic differences with respect to spectroscopic subtypes. The total DA to non-DA ratio of the 25 pc sample is 1.8, a manifestation of deepening envelope convection, which transforms DA stars with sufficiently thin H surface layers into non-DAs. We compare this ratio with the results of other studies. We find that at least 11% of the WDs within 25 pc of the Sun (the DAZ and DZ stars) have photospheric metals that likely originate from accretion of circumstellar material (debris disks) around them. If this interpretation is correct, then it suggests the possibility that a similar percentage have planets, asteroid-like bodies, or debris disks orbiting them. Our volume-limited sample reveals a pileup of DC WDs at the well-known cutoff in DQ WDs at $T_{\rm eff} \sim 6000$ K. Mindful of small number statistics, we speculate on its possible evolutionary significance. We find that the incidence of magnetic WDs in the 25 pc sample is at least 8% in our volume-limited sample, dominated by cool WDs. We derive approximate formation rates of DB and DQ degenerates and present a preliminary test of the evolutionary scenario that all cooling DB stars become DQ WDs via helium convective dredge-up with the diffusion tail of carbon extending upward from their cores.

Key words: stars: evolution – stars: kinematics and dynamics – stars: statistics – techniques: photometric – techniques: spectroscopic – white dwarfs

1. INTRODUCTION

Extending the census of local white dwarfs (WDs) to increasingly large volumes of space around the Sun offers a plethora of crucial astrophysical insights, including (1) identification of the lowest luminosity, hence oldest, WDs in the immediate neighborhood of the Sun; (2) the distribution of WD spectroscopic subgroups and their mix of progenitor stellar populations; (3) a direct measurement of the local space density and mass density of WDs; and (4) a window into the history of star formation and stellar evolution in the Galactic plane as well as the age constraint of the Galactic disk (Liebert et al. 1988; Oswalt et al. 1996) by enabling the determination of the cool WD luminosity function. The sample of WDs out to 20 pc was presented by Holberg et al. (2008b) and Sion et al. (2009), who utilized available temperatures, gravities, and spectral types from the literature to attempt a full characterization of the local sample of WDs. With the publication of new atmospheric parameters and more accurate distances for a larger sample of local WDs out to 25 pc, the statistical and kinematical properties of the volume-limited sample of local WDs merit re-examination.

The local 25 pc WD sample is a well characterized, volume-limited population with a high degree of completeness. It contains a sample of 224 WDs including double degenerate systems. While it has an overall completeness of 65%, the 20 pc and 13 pc samples have completenesses of 85% and 100%, respectively. As such, it lends itself to a number of analyses that can be used to anchor larger, less complete spectroscopic and photometric surveys that are not volume-limited. The results of the current 25 pc sample will be discussed in J. Holberg et al. (2014, in preparation), which will include an evaluation of the spatial distribution, the space density, and the completeness of the sample, as well as the mass distribution, local luminosity function, and binary fraction.

In this paper, we discuss the kinematics and the distribution of WD temperature and spectroscopic subtypes in the 25 pc sample around the Sun, and propose tests of scenarios of cool WD spectral evolution. We briefly describe the enhanced 25 pc sample in Section 2. The kinematic properties of this sample are discussed in Section 3. The DQ and DC components of the 25 pc sample and their temperature distributions are discussed in Section 4. The magnetic and cool DZ stars are discussed in Sections 5 and 6, respectively. In Section 7 we describe preliminary tests of cool WD spectral evolution using the volume-limited 25 pc sample. Section 8 contains our conclusions.

2. CENSUS OF WHITE DWARFS OUT TO 25 pc

Table 1 presents the sample of WDs within 25 pc of the Sun. The basic observational data with which we examined the distribution of WD spectral types and the data used for space motions are given in Table 1, which contains by column: (1) the WD number, (2) the coordinates (R.A. and decl. are in decimal degrees), (3) $T_{\rm eff}$, (4) DIST (distance in parsecs), (5) PM (proper motion in arcsec yr^{-1}), (6) PA (position angle in degrees), (7) the method of distance determination, denoted by *p* for trigonometric parallax and *s* for spectrophotometric distances, and (8) a reference abbreviation to the bibliography. Many of the distances are obtained from trigonometric parallaxes, the remainder from spectrophotometric distances.

A substantial fraction of the data in Table 1 was taken from the detailed survey of the local WDs out to 20 pc by Holberg et al. (2008b) and Sion et al. (2009). To this sample of 129 WDs,

Table 1
Observational Data Used in Space Motions

WD	Type	$T_{\rm eff}$	R.A.	Decl.	DIST	PM	PA	Method	Ref.
0000−345	DCP8.1	6643	000.667	−34.222	13.21	0.7578	169.046	p	L20
0008+424	DA6.8	7380	002.843	+42.678	22.00	0.2328	191.648	sp	L20
0009+501	DAH7.6	6502	003.061	+50.422	11.03	0.7150	219.920	p	L20
0011−134	DAH8.4	5992	003.553	−13.183	19.49	0.8990	217.337	p	L20
0011−721	DA7.8	6325	003.457	−71.831	···	0.3260	141.300	sp	GBD
0029−031	DA11.3	4470	008.041	−02.900	23.47	0.6505	76.305	p	pi
0038+555	DQ4.6	10900	010.337	+55.834	23.04	0.3396	103.627	p	pi
0038−226	DQpec9.3	5529	010.358	−22.350	9.04	0.6047	232.600	p	L20
0046+051	DZ7.4	6215	012.291	+05.388	04.31	2.9780	155.538	p	L20
0053−117	DA7.1		13.959	−11.458	···	0.4396	350.045	sp	G11
0108+048	DA6.4	8530	015.958	+05.075	21.32	0.3924	053.393	p	G11
0108+277	DA9.6	6428	017.686	+27.970	13.8	0.2270	219.321	p	L20
0115+159	DQ5.6	9119	019.500	+16.172	15.40	0.6480	181.805	p	L20
0121−429	DAH7.9	6299	021.016	−42.677	18.31	0.5941	151.000	p	L20
0123−262	DC6.9		021.351	−26.012	···	0.5945	154.8143	sp	GBD
0123−460	DA8.5	5898	021.325	−45.752	24.90	0.7483	136.299	sp	Sub08
0134+883	DA2.8	18311	025.369	+83.583	25.60	0.1500	306.870	sp	G11
0135−052	DA6.9	7118	024.497	−04.995	12.34	0.6810	120.838	p	L20
0141−675	DA7.8	6248	025.754	−67.308	09.72	1.0797	199.000	p	L20
0145+360	DA7.8	6470	27.168	+36.258	24.2	···	···	sp	Lim
0148+467	DA3.8	14005	028.012	+47.001	15.85	0.1240	0.569	p	L20
0148+641	DA5.6	9016	027.963	+64.431	17	0.2854	123.857	sp	DR7
0208+396	DAZ6.9	7264	032.836	+39.922	16.72	1.1450	115.746	p	L20
0210−508	DQ+K1	6000	032.608	−50.823	10.91	2.1920	72.666	p	SL
0213+396	DA5.4		034.068	39.857	···	0.1873	239.876	sp	G11
0213+427	DA9.0	5507	034.281	+42.977	19.92	1.0470	125.065	p	n L20
0227+050	DA2.7	18779	037.569	+05.264	24.30	0.0783	107.764	p	G11
0230−144	DA9.2	5477	038.157	−14.197	15.62	0.6870	177.114	p	L20
0231−054	DA3.7	13550	038.532	−05.194	22.7	0.2655	69.722	sp	GBR11
0233−242	DC9.3	5312	038.840	−24.013	15.3	0.6220	189.015	sp	L20
0236+259	DA9.2	5500	039.832	+26.165	21.00	0.3591	117.35	p	Pi
0243−026	DAZ7.4	6839	041.628	−02.456	21.23	0.5342	155.21	p	G11
0245+541	DAZ9.5	5319	042.151	+54.389	10.35	0.5735	227.827	p	L20
0252+497	DA7.9	6370	···	···	16.7	···	···	sp	Lim
0255−705	DAZ4.7	10560	044.071	−70.369	21	0.6596	99.776	sp	G11
0310−688	DA3.3	16865	047.628	−68.600	10.15	0.1112	158.097	p	L20
0311−649	DA4.0	11945	048.107	−64.736	21.00	0.1661	101.107	sp	Sub08
0322−019	DAZ9.9	5195	051.296	−01.820	16.80	0.9090	164.625	p	L20
0326−273	DA5.4	8483	052.203	−27.317	17.36	0.8503	071.629	p	L20
0340+198	DA7.0	7160	055.846	19.970	18.4	0.178	24.55	sp	Lim
0341+182	DQ7.7	6568	056.145	+18.436	19.01	1.1990	159.771	p	L20
0344+014	DC9.9	5170	056.778	+01.646	···	0.4730	150.400	sp	L20
0357+081	DA9.2	5478	060.111	+08.235	17.82	0.5352	222.274	p	L20
0413−077	DA3.1	17100	063.839	−07.656	05.04	4.0880	213.216	p	L20
0416−594	DA3.3	14000	064.122	−59.302	18.23	0.1740	195.838	p	SL
0419−487	DA8	6300	065.273	−48.652	20.12	0.5402	178.302	p	G11
0423+044	DA	5140	066.658	+04.541	20.72	0.8469	131.936	p	Pi
0423+120	DA8.2	6167	066.473	+12.196	17.36	0.2446	335.866	p	L20
0426+588	DC7.1	7178	067.797	+58.977	05.53	2.4267	147.602	p	L20
0431−279	DC9.5	5330	068.390	−27.890	24.7	0.388	90.738	p	Sub08
0431−360	DA10.0	5153	068.232	−35.395	25.0	0.301	84.1	sp	Sub08
0433+270	DA9.0	5629	069.187	+27.164	17.85	0.2760	124.196	p	L20
0435−088	DQ8.0	6367	069.447	−08.819	09.50	1.5740	171.103	p	L20
0454+620	DA4.3	11610	24.663	+62.152	24.9	0.188	149.6	sp	Lim
0457−004	DA4.7	10800	074.930	−00.377	21.93	0.2926	142.778	sp	L20
0503−174	DAH9.5	5300	076.498	−17.378	20.27	0.6876	14.4	p	Pi
0511+079	DA7.7	6590	078.514	+08.004	20.26	0.3642	216.178	p	G11
0532+414	DA6.8	7739	084.084	+41.498	23.81	0.1668	284.903	sp	G11
0548−001	DQP8.3	6070	087.831	−00.172	11.07	0.2510	025.810	p	L20
0552−041	DZ10.0	5182	088.789	−04.168	06.41	2.3760	166.600	p	
0553+053	DAP8.7	5785	089.106	+05.363	07.99	1.0272	204.993	p	L20
0615−591	DB3.2	16714	094.063	−59.206	23.80	0.379	166	p	Pi
0618+067	DA8.1	5940	095.198	+06.754	22.62	0.5352	91.392	p	G11
0620−402	DZ6	5919	095.423	−40.217	21.50	0.379	166	p	L20
0628−020	DA	6912	097.661	−02.097	21.50	0.2088	253.300	p	G11
0642−166	DA2	25967	101.288	−16.713	02.63	1.3394	204.057	p	L20

Table 1
(Continued)

WD	Type	$T_{\rm eff}$	R.A.	Decl.	DIST	PM	PA	Method	Ref.
0644+025	DA6.8	22288	101.842	+02.519	18.45	0.4234	272.572	p	L20
0644+375	DA2.4	22288	101.908	+37.515	15.40	0.9624	193.561	p	L20
0649+639	DA8.1	6230	103.560	+63.932	21.1	0.200	225.0	sp	Lim
0651−398A	DA7.0	7222	103.397	−39.925	25.10	0.2125	341.906	sp	Sub08
0655−390	DA7.9	6311	104.274	−39.159	17.2	0.3400	242.600	sp	GBD
0657+320	DA10.1	4888	105.215	+31.962	18.69	0.6910	149.362	p	L20
0659−063	DA7.7	6627	105.478	−06.463	12.34	0.8984	184.981	p	L20
0706+377	DQ7.6	6590	107.559	+37.672	24.27	0.3577	220.010	p	Pi
0708−670	DC9.9	5097	107.217	−67.108	17.5	0.2460	246.300	sp	GBD
0727+482.1	DA10.0	4934	112.678	+48.199	11.11	1.2868	190.070	p	L20
0727+482.2	DA10.1	4926	112.697	+48.173	11.11	1.2868	190.070	p	L20
0728+642	DAP11.1	5135	113.378	+64.157	13.4	0.2660	171.352	sp	L20
0736+053	DQZ6.5	7871	114.827	+05.227	03.50	1.2590	214.574	p	L20
0738−172	DZA6.6	7650	115.086	−17.413	09.09	1.2634	116.600	p	L20
0743−336	DC10.6	4462	116.410	−33.931	15.19	1.7360	352.670	p	L20
0744+112	DA6.2	8160	116.875	11.126	25.7	0.1907	161.66	sp	Lim
0747+073.1	DC10.4	4366	117.563	+07.193	18.28	1.8049	173.414	p	L20
0747+073.2	DC12.0	4782	117.560	+07.196	18.28	1.8049	173.414	p	L20
0749+426	DC11.7	4585	118.305	+42.500	17.8	0.420	165.845	sp	L20
0751−252	DA9.8	5085	118.485	−25.400	17.68	0.3622	304.700	p	L20
0752−676	DA8.8	5735	118.284	−67.792	07.89	2.1499	135.867	p	L20
0753+417	DA7.3	6880	119.129	+41.664	24	0.3481	181.316	sp	Kilic-10
0805+356	DA7.3	6900	122.296	+35.465	21.1	0.1051	220.873	sp	Trem11
0806−661	DQ4.9	10205	121.723	−66.304	19.16	0.4468	130.400	p	L20
0810+489	DC6.9	7300	123.546	+48.758	17.00	0.258	166.5	p	GBD
0816−310	DZ7.6	6463	124.667	−31.172	23.80	0.8163	164.074	sp	GBD
0821−669	DA9.8	5088	125.361	−67.055	10.65	0.7623	329.500	p	L20
0827+328	DA6.9	7490	127.664	+32.696	22.27	0.5412	196.090	p	L20
0839−327	DA5.5	9081	130.384	−32.942	08.81	1.7020	322.700	p	G11
0840−136	DZ10.3	4874	130.701	−13.786	19.3	0.2720	263.000	sp	L20
0843+358	DZ6	9041	131.685	+35.642	23.1	0.174	244.466	sp	GBD
0856+331	DQ5.1	9920	134.811	+32.953	20.49	0.334	269.657	p	Pi
0912+536	DCP7	7235	138.983	+53.423	10.30	1.5630	223.997	p	L20
0946+534	DQ6.2	8100	147.571	+53.254	22.98	0.2642	259.753	p	Pi
0955+247	DA5.8	8621	149.451	+24.548	24.44	0.4200	219.848	p	L20
0959+149	DC7	7200	150.455	+14.689	22.2	0.339	269.493	p	GJ
1008+290	DQpec11.0		152.923	28.766	···	0.7201	189.593	p	Pi
1009−184	DZ8.5	6036	153.007	−18.725	18.30	0.5114	269.000	p	L20
1012+083.1	DA7.5	6750	153.760	+08.109	25.80	0.3339	300.405	sp	G11
1019+637	DA7.2	6742	155.787	+63.461	16.33	0.3790	053.160	p	L20
1033+714	DC10.3	4727	159.260	+71.183	15.15	1.9170	256.008	p	L20
1036−204	DQpecP10.2	4694	159.731	−20.682	14.28	0.6100	334.000	p	L20
1043−188	DQ8.1	5780	161.412	−19.114	12.15	1.9780	251.636	p	L20
1055−072	DA6.8	7491	164.396	−07.523	13.42	0.8270	276.328	p	L20
1105−048	DA3.5	15141	166.999	−05.157	24.2	0.4445	188.148	sp	G11
1116−470	DC8.6	5801	169.613	−47.365	17.9	0.3220	275.100	sp	GBD
1121+216	DA6.7	7434	171.054	+21.359	13.42	1.0400	269.240	p	L20
1124+595	DA4.8	10747	171.718	+59.321	25	0.1569	108.204	sp	L20
1132−325	DC		173.623	−32.832	09.53	0.9400	038.955	p	L20
1134+300	DA2.4	22469	174.271	+29.799	15.31	0.1480	267.948	p	L20
1142−645	DQ6.4	7966	176.458	−64.841	04.62	2.6876	097.500	p	L20
1148+687	DA7.6	···	177.718	+68.521	16.8	···	···	sp	DR7
1149−272	DQ8.1	6200	177.900	−27.539	24.40	0.229	283.126	sp	Sub08
1202−232	DAZ5.8	8767	181.361	−23.553	10.82	0.2458	16.600	p	L20
1208+576	DAZ8.6	6200	182.872	+57.404	20.44	0.5486	132.414	p	G11
1214+032	DA8.0	6272	184.216	+02.968	19.72	0.6947	291.357	sp	Pi
1223−659	DA6.6	7594	186.625	−66.205	16.25	0.1858	186.900	p	G11
1236−495	DA4.3	11599	189.708	−49.800	16.39	0.4902	255.709	p	L20
1241−798	DC/DQ	9556	191.219	−80.157	22.10	0.5524	309.858	sp	Sub08
1242−105	DA6.3		191.219	−10.852	···	0.3488	257.079	sp	GBD
1257+037	DA9.0	5616	195.037	+03.478	16.58	0.9696	206.195	p	L20
1309+853	DAP9	5440	197.171	+85.041	16.47	0.3213	140.811	p	L20
1310+583	DA4.8	10544	198.241	+58.086	21.1	0.1995	112.708	sp	G11
1310−472	DC11.9	4158	198.248	−47.468	15.03	2.2047	105.253	p	L20
1315−781	DC8.8	5619	199.856	−78.391	19.17	0.4700	139.5	p	Pi
1327−083	DA3.6	14571	202.556	−08.574	16.86	1.2049	246.761	p	L20

Table 1
(Continued)

WD	Type	$T_{\rm eff}$	R.A.	Decl.	DIST	PM	PA	Method	Ref.
1334+039	DA11	4971	204.132	+03.679	08.23	3.8800	252.775	p	L20
1344+106	DAH7.1	7059	206.851	+10.360	20.04	0.9032	260.569	p	L20
1337+705	DAZ2.5	20464	204.710	+70.285	24.79	0.405	266.035	p	G11
1338+052	DC11.6		205.340	5.012	···	0.438	271.6	sp	Say
1339−340	DA9.5	5361	206.508	+57.009	21.20	0.2758	315.881	sp	GBD
1344+572	DA3.8	13389	206.510	+57.008	20	0.273	315.9	sp	G11
1345+238	DA11	4581	207.012	+23.579	12.06	1.4960	274.637	p	L20
1350−090	DAP5	9518	208.314	−09.275	22.73	0.3618	174.226	sp	G11
1401+457	DC19	2600	210.853	+45.558	24.00	0.2840	251.947	sp	Kilic$_{10}$
1425−811	DAV4.2	12098	218.282	−80.157	22.72	0.5524	201.418	p	G11
1436−781	DA8.1	6270	220.714	−78.398	24.65	0.4096	275.1	p	Pi
1444−174	DC10.2	4982	221.855	−17.704	14.49	1.1440	252.643	p	L20
1532+129	DZ6.7	7500	233.774	+12.795	22	0.2464	222.039	sp	Koe$_{11}$
1538+333	DA5.6	8940	235.139	+33.147	22.72	0.186	296.152	p	Pi
1542−275	DB4.0		237.658	27.656	···	0.246	235.9	sp	Ber11
1544−377	DA4.8	10610	236.875	−37.918	15.24	0.4685	242.838	p	L20
1609+135	DA5.4	9041	242.856	+13.371	18.34	0.5510	178.513	p	L20
1620−391	DA2.1	25985	245.890	−39.229	12.86	0.0755	89.962	p	L20
1625+093	DA7.3	7038	246.972	+09.204	23.36	0.4872	192.325	p	G11
1626+368	DZA6.0	8507	247.104	+36.771	15.94	0.8881	326.668	p	L20
1630+089	DA9.0	5640	177.717	+68.521	13.2	0.4	···	sp	Lim
1632+177	DAZ5.0	10225	248.674	+17.609	···	0.0885	108.435	sp	L20
1633+433	DAZ7.7	6608	248.755	+43.293	15.10	0.3730	144.151	p	L20
1633+572	DQ8.2	5958	248.589	+57.169	14.45	1.6440	317.229	p	L20
1639+537	DAH6.7	7510	250.238	+53.685	21.09	0.2369	212.416	p	Pi
1647+591	DAV4.1	12738	252.106	+59.056	10.95	0.3236	154.498	p	L20
1655+215	DAB5.4	9179	254.291	+21.446	23.25	0.5820	178.040	p	L20
1658+440	DAP1.7	30510	254.951	+44.017	22.00	0.1012	341.869	sp	G11
1705+030	DZ7.7	6584	257.033	+02.960	17.54	0.3790	180.907	p	L20
1748+708	DQ9.0	5570	267.033	+70.876	06.07	1.6810	311.394	p	L20
1756+143	DA9.0	5466	269.595	+14.293	22.40	1.0054	235.045	sp	GBD
1756+827	DA6.9	7214	267.458	+82.773	15.64	3.5897	336.542	p	L20
1814+134	DA9.5	5251	274.277	+13.473	14.22	1.2070	201.500	p	L20
1817−598	DA5.8	4960	275.497	−59.863	24.87	0.3653	194.911	p	Pi
1820+609	DA10.5	4919	275.332	+61.018	12.78	0.7133	168.517	p	L20
1829+547	DQP8.0	6345	277.584	+54.790	14.97	0.3991	317.234	p	L20
1840+042	DA5.8	9090	280.857	+04.339	24.87	0.187	296.935	p	G11
1900+705	DAP4.2	11835	285.042	+70.664	12.98	0.5064	10.467	p	L20
1911+536	DA2.9	17670	288.202	+53.720	22.1	0.018	225.0	sp	Lim
1912+143	DA7.3	6940	288.650	+14.473	19.4	0.161	225.0	sp	Lim
1917+386	DC7.9	6459	289.744	+38.722	11.69	0.2510	174.028	p	L20
1917−077	DBQZ4.9	10396	290.145	−07.666	10.08	0.1740	200.602	p	L20
1919+145	DA3.3	15280	290.418	+14.678	19.80	0.0743	203.806	p	L20
1935+276	DA4.2	12130	294.307	+27.721	17.95	0.4361	088.686	p	L20
1953−011	DC6.4	7920	299.121	−01.042	11.38	0.8270	212.314	p	L20
2002−110	DA10.5	4800	301.395	−10.948	17.33	1.0740	095.523	p	L20
2007−303	DA3.5	14454	302.736	−30.218	17.09	0.4280	233.492	p	L20
2008−600	DC9.9	5080	303.132	−59.947	16.55	1.4276	166.100	p	L20
2008−799	DA8.5	5800	304.207	−79.764	24.96	0.4339	127.979	p	Pi
2011+065	DQ7	6400	303.481	+06.712	22.37	0.6297	203.39	p	Pi
2032+248	DA2.4	19983	308.591	+25.063	14.65	0.6920	215.554	p	L20
2039−202	DA2.5	19207	310.644	−20.076	21.10	0.3672	104.831	p	G11
2039−682	DA3.1	15855	311.089	−68.089	22.00	0.3269	144.462	sp	G11
2040−392	DA4.5	10830	310.955	−39.055	22.63	0.306	179	p	G11
2047+372	DA3.6	14070	312.277	+37.470	17.28	0.2190	047.150	p	L20
2048+263	DA9.7	5200	312.586	+26.511	20.08	0.5149	235.044	p	L20
2048−250	DA6.6	7630	312.749	−24.867	22	0.2776	129.885	sp	GBD
2054−050	DC10.9	4620	314.199	−04.844	17.05	0.8020	106.562	p	L20
2058+342	DB4.1		315.089	34.439	···	0.168	42.6	sp	Ber11
2105−820	DA4.7	10620	318.320	−81.820	17.06	0.5164	146.372	p	L20
2111+072	DA7.8	6470	317.370	+07.451	24.1	0.341	70.289	sp	Lim
2115−560	DA6	9736	319.902	−55.837	22.00	0.4652	115.463	sp	G11
2117+539	DA3.6	13990	319.734	+54.211	19.72	0.2130	336.371	p	L20
2118−388	DC9.6	5244	320.523	−38.643	22.00	0.1786	112.009	sp	Sub08
2119+040	DA9.0		320.551	4.232	···	0.3897	28.341	sp	Say
2126+734	DA3.8	16,104	321.740	73.645	21.23	0.2915	171.119	p	G11

Table 1
(Continued)

WD	Type	$T_{\rm eff}$	R.A.	Decl.	DIST	PM	PA	Method	Ref.
2133−135	DA5.0	9736	324.068	−13.309	20.40	0.2935	118.486	sp	Sub08
2138−332	DZ7	7240	325.489	−33.008	15.62	0.2100	228.500	p	L20
2140+207	DQ6.1	8200	325.670	+20.999	12.51	0.6819	199.445	p	L20
2149+021	DA2.8	17353	328.105	+02.388	24.50	0.3003	177.328	p	G11
2151−015	DA6	8400	328.526	−01.285	19.60	0.2851	178.191	sp	G11
2154−512	DQ8.3	6100	329.421	−51.006	16.12	0.3746	184.738	p	L20
2159−754	DA5.6	9040	331.086	−75.223	15.62	0.2042	238.300	p	L20
2210+565	DA3.0	16790	332.973	+56.829	18.1	0.147	217.0	sp	Say
2211−392	DA8.1	6920	333.638	−38.983	18.69	1.068	109.6	p	Say
2211−392	DA8.1	6920	333.644	−38.985	18.79	1.0560	110.100	p	Say
2215+386	DC10.6	4700	334.448	+37.130	25.12	0.4691	78.69	p	Pi
2226−754	DC11.9	4230	337.665	−75.232	12.8	1.8680	167.500	sp	L20
2226−755	DC12.1	4177	337.638	−75.255	14.0	1.8680	167.500	sp	L20
2246+223	DA4.7	10647	342.273	+22.608	19.04	0.5253	83.551	p	L20
2248+293	DA9	5580	342.845	+29.662	20.92	1.2575	83.745	p	G11
2251−070	DZ12.6	4000	343.472	−06.781	08.51	2.5718	105.600	p	L20
2253+054	DA9	5600	343.982	+05.755	24.46	0.4471	127.101	p	Pi
2311−068	DQ6.8	7440	348.604	−06.546	25.1	0.3815	244.039	p	Pi
2322+137	DA10.7	4700	351.332	+14.060	22.27	0.37	71.565	p	L20
2326+049	DAV4.3	12206	352.198	+05.248	13.62	0.4934	236.406	p	G11
2336−079	DA4.6	10938	354.711	−07.688	15.94	0.0500	140.000	p	L20
2341+322	DA4.0	13128	355.961	+32.546	17.60	0.2290	252.150	p	L20
2347+292	DA9	5810	357.479	+29.567	22.39	0.5065	185.666	p	Pi
2351−335	DA5.7	8850	358.504	−33.275	23.35	0.5081	219.4	p	G11
2359−434	DA5.9	8648	000.544	−43.165	08.16	0.8878	138.400	p	L20

Notes. s, spectrophotometric; p, trigonometric parallax; a, weighted mean average.
References. G11: Gianninas et al. (2011); Lim: Limoges et al. (2013); Say: Sayres et al. (2012); Pi: Trig. Parallax; DR7: J. Holberg et al. (2014, in preparation); Sub08: Subasavage et al. (2008); GBR11: Gianninas et al. (2011); Sub07: Subasavage et al. (2007); Ber11: Bergeron et al. (2011); GJ: Gliese & Jarheise (1995); Kilic10: Kilic et al. (2010); Koe11: Koester et al. (2011); Trem11: Tremblay et al. (2011).

Table 2
Distribution of WD Spectral Subtypes within 25 pc

Spectral Type	Range of $T_{\rm eff}$	Number of Stars	% of Total
DA	4590–25193	125	54%
DAZ	5093–20464	11	5%
DAH/DAP	4500–30510	14	6%
Magnetic Non-DA		5	
DB	16714	2	0.8%
DBQZ	10200	1	0.4%
DC	2600–7300	28	12%
DCP	6010	3	1.3%
DQ	5590–10900	23	8%
DQP	4948–6070	3	0.9%
DQZ	7740	1	0.4%
DZ	4000–7500	13	5%
DZA	7600–8440	2	0.9%

we have added 95 WDs out to a volume of 25 pc radius, giving a total sample of 224 WDs including double degenerates known out to 25 pc. As in Holberg et al. (2008b) and Sion et al. (2009), the photometric distances were computed based on spectroscopic and photometric measurements following the methods described in Holberg et al. (2008a). Proper Motions are taken from the McCook and Sion Catalog, or where available, were determined from NOMAD. Radial velocities were available from the literature for approximately 50% of our sample, and correspond either to direct measurements of the WD, or the system velocities or radial velocities of the main sequence companions (McCook & Sion 1999 and references therein; Maxted et al. 2000; Silvestri et al. 2001, 2002; Pauli et al. 2003, 2006). For radial velocities derived from individual WDs, we applied corrections for the gravitational redshift based on the individual masses and radii of each star. These mass and radius determinations were interpolated from within the synthetic photometric tables described in Holberg & Bergeron (2006) and were based on temperatures and gravities given in Holberg et al. (2008b, hereafter, LS08). Using the spectral types and temperatures given in LS08 and Holberg (2008), we assembled the local population of WDs lying within 25 pc of the Sun using a number of compilations, including Gliese & Jarheise (1995), LS08, Sion et al. (2009), Sayres et al. (2012), Bergeron et al. (2011), Giammichele et al. (2012), Dufour et al. (2007), Limoges et al. (2013), Subasavage et al. (2007, 2008), Gianninas et al. (2011), Kilic et al. (2010), Koester et al. (2011), and Tremblay et al. (2011).

We summarize the percentage breakdown of spectral subtypes among the 25 pc sample of local WDs in Table 2. As expected, the DA stars dominate the sample. If we take the total DA sample to include DAZ stars and magnetic DA stars, then there are 150 DA stars within 25 pc.

In Figure 1 we display a histogram with the number versus $T_{\rm eff}$ distribution function of DA stars in the lower panel and non-DA stars in the upper panel. The skewing of their distribution toward lower temperatures not only reflects the predominance of cool DAs and cool non-DAs in a sample so close to the Sun, but the variation of this ratio, DA/non-DA, as a function of $T_{\rm eff}$, also holds key physical significance to our understanding of WD spectral evolution.

The overall DA to non-DA ratio of the 25 pc sample is 1.83. This is a slightly larger ratio than found in the 20 pc sample and is likely a lower limit since a few of the cool non-DAs (especially DC stars) may actually prove to be H-dominated. Sion (1984)

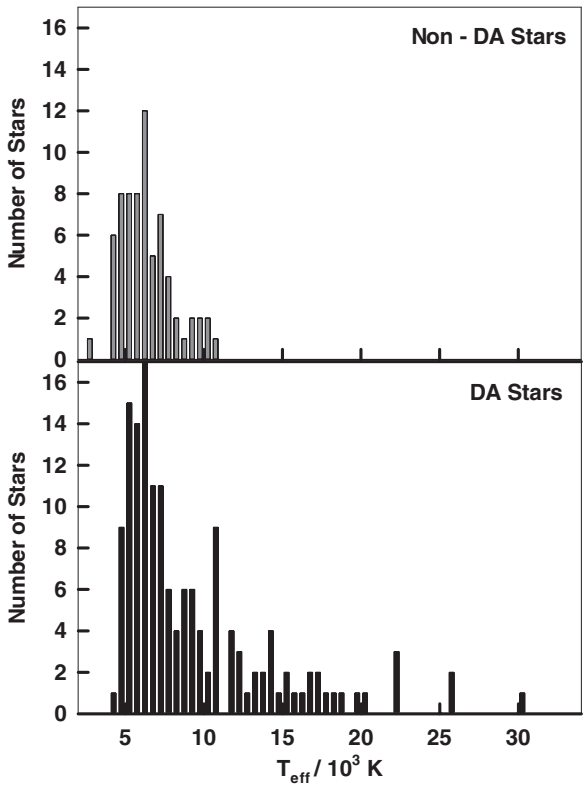

Figure 1. Histogram of the number vs. surface temperature distribution function for all DA white dwarfs (lower panel) and all non-DA white dwarfs (upper panel) within 25 pc of the Sun.

uncovered the first empirical evidence of this transformation of WD surface compositions and attributed the lowering of the DA/non-DA ratio with decreasing $T_{\rm eff}$ to the mixing and dilution of hydrogen into the deepening helium convection zone (Sion 1984; see also Greenstein 1986). Sion (1984) estimated that this convective mixing away of surface hydrogen in cooling DA stars occurs at $T_{\rm eff} \sim$ 10–12,000 K. Subsequent more detailed work with evolutionary models (Tremblay & Bergeron 2008; Bergeron et al. 2001), using a larger, more homogenous sample of WDs, presented a more complex picture of spectral evolution at temperatures below 15,000 K. They showed that as a DA WD cools, the bottom of the hydrogen convection zone eventually reaches the helium convection zone but only if the hydrogen layer is thin enough, with the actual temperature at which the conversion occurs depending on the thickness of the hydrogen layer. In other words, DA WDs with thicker hydrogen layers will mix at lower $T_{\rm eff}$. They showed that the H layer mass that would mix at a given temperature depends on the assumed convective efficiency, with ∼85% of all DA stars between 10,000 K and 15,000 K having hydrogen layer masses large enough for them to remain recognized as DA stars down to 8000 K. It is clear from the results of Tremblay & Bergeron (2008) that the details of WD spectral evolution remain murky below 12,000 K. This can only be clarified with further theoretical modeling predictions confronted by ever larger samples of cool WDs with high quality spectra.

3. KINEMATICS OF THE LOCAL WHITE DWARFS

The vector components of the space motions are U, V, and W, where U is positive in the direction of the galactic anti-center, V is positive in the direction of the galactic rotation, and W is positive in the direction of the north Galactic pole (Wooley et al. 1970). The U, V, and W components and total motions were computed along with the average velocities and velocity dispersions for the different spectroscopic subtypes in the 25 pc sample in Table 1. In Table 3, we present the computed vector components of the space motion for each WD in Table 1. We note that for some of the WDs in Table 1, there are two sets of space motions from slightly different input parameters, such as proper motion and position angles. For these objects, two different sets of U, V, W, T values were computed and used to compute the averages and dispersions tabulated in Table 4. These mean velocities and velocity dispersions reveal no clear evidence that different spectral subtypes have significantly different space motions.

If we take $T > 150$ km s^{-1} as the lower cutoff for halo space motions, then there are seven stars or 3% of the total sample that have possible halo Population II stars in extreme galactic orbits that could happen to be interlopers in the solar neighborhood. These objects are WD0747+482.1 (DC10.4; 156 km s^{-1}), WD0747+482.2 (DC12.0; 156 km s^{-1}), WD0959+149 (DC7; 144 km s^{-1}), WD1310−472 (DC11.9; 166 km s^{-1}), WD1334+039 (DA11.0; 151 km s^{-1}), WD1339−340 (DA9.5; 215 km s^{-1}), and WD1756+827 (DA6.9; 156 km s^{-1}).

To further investigate the question of population membership, we point out that the assignment of reliable population membership for local WDs must involve not only the vector components of the space motion but also the cooling ages derived from their surface temperatures and total stellar age. In contrast, the population membership of main sequence stars utilizes kinematical characteristics as well as chemical abundance data, e.g., metallicity. Despite this difference in the way population membership is assigned for the two types of stars, it is useful to compare the velocity distribution of the WD sample in the U versus V velocity plane with the velocity distribution (velocity ellipsoids) characterizing a well-studied sample of main sequence stars (Chiba & Beers 2000; Sion et al. 2009).

However, a halo or thick disk member star cannot be identified on the basis of kinematic data alone. The candidate star must also have a total stellar age that is of the order of 12 billion years or older. The temperature of the six stars given in Table 1 indicates cooling ages well below 12 billion years. Thus, their space motions together with their total stellar ages lead to the conclusion that there is no clear evidence of halo WDs among the WDs within 25 pc of the Sun.

In Figure 2, we display the U versus V space velocity diagram for the 25 pc sample of WDs, with the assumption of zero radial velocity, relative to velocity ellipses for main sequence stars (Chiba & Beers 2000; see also Kawka & Vennes 2006; Sion et al. 2009). DA stars are denoted by closed circles, while non-DA stars are denoted by closed triangles. In the diagram, the 2σ velocity ellipse contour (denoted by the solid line) of the thin disk component is displayed, as well as the 2σ ellipse of the thick disk component (short-dashed line) and the 1σ contour of the halo component (long-dashed line). The vast majority of WDs lie within the thin disk, as expected for the local sample. However, we see that nearly equal small numbers of DAs and non-DAs lie outside the thin disk ellipsoid but within the thick disk ellipse, while three stars, two DAs and one non-DA, lie clearly within the halo velocity ellipse. Finally, one non-DA and two DA stars have anomalous velocities, placing them at very large positive V velocity components.

Given the concentric, nested nature of the thin and thick disk velocity ellipses in the $U - V$ plane, it is difficult to clearly disentangle the two populations. Age is a strong discriminate,

Table 3
Space Motions of White Dwarfs within 25 pc

WD No.	Type	U	V	W	T
0000−345	DCP9	−11.9	−43.7	3.2	45.4
0008+424	DA6.8	−10.0	−1.9	−17.4	20.2
0009+501	DAH7.7	−28.1	8.6	−24.1	38.0
0011−134	DCH8.4	−75.5	−31.1	−9.8	82.3
0011−721	DA8.0	10.3	−23.2	12.2	28.2
0029−031	DA11.3	68.3	−23.0	2.6	72.1
0038+555	DQ4.6	39.4	−2.0	−11.9	41.2
0038−226	DQ9.3	−24.9	−4.6	−1.2	25.3
0046+051	DZ8.1	−2.8	−53.6	−30.3	61.6
0108+048	DA6.4	38.2	−0.1	11.8	40.0
0108+277	DAZ9.6	−11.9	0.3	−9.9	15.5
0115+159	DQ6	−21.4	−27.2	−32.0	47.2
0121−429	DAH7.9	−0.7	−46.8	11.1	48.1
0123−460	DA8.5	24.3	−91.0	24.9	97.4
0134+883	DA2.8	−11.1	5.1	6.1	13.7
0135−052	DA6.9	16.8	−37.2	−1.6	40.9
0141−675	DA7.8	−21.8	−22.8	21.5	38.2
0148+467	DA3.8	2.6	1.8	8.3	8.8
0148+641	DA5.6	12.3	−11.2	−6.8	18.0
0208+396	DAZ7.0	43.0	−62.9	−6.7	76.5
0210−510	DA10	85.6	−42.1	24.0	98.4
0213+427	DA9.4	37.8	−67.3	−19.8	79.8
0227+050	DA2.7	−0.1	−8.9	7.1	11.4
0230−144	DC9.5	−20.7	−43.3	−13.3	49.9
0231−054	DA3.7	68.5	−6.7	−56.4	89.0
0233−242	DC9.3	−24.2	−34.1	−9.8	43.0
0236+259	DA9.2	29.1	−21.1	−8.9	37.0
0243−026	DAZ7.4	8.9	−51.6	−34.5	62.7
0245+541	DAZ9.7	−16.4	10.9	−24.2	31.3
0255−705	DAZ4.7	22.2	−82.0	−0.6	84.9
0310−688	DA3.1	0.1	−4.2	2.8	5.1
0311−649	DA4.0	7.9	−12.8	9.5	17.8
0322−019	DAZ9.7	−21.5	−66.8	−20.7	73.2
0326−273	DA5.4	46.7	−29.7	47.2	72.8
0341+182	DQ7.7	−16.0	−94.9	−23.8	99.1
0344+014	DQ9.9	−7.9	−43.8	−4.9	44.8
0357+081	DC9.2	−25.3	−4.3	−36.8	44.9
0413−077	DAP3.1	−44.2	−34.8	−73.0	92.2
0419−487	DA8	−1.2	−91.1	−57.4	107.7
0416−594	DA3.8	−4.9	−5.7	−1.6	7.7
0423+044	DA9	−6.9	−80.5	17.2	82.6
0423+120	DA8.2	5.3	18.1	3.8	19.3
0426+588	DC7.1	0.9	−35.4	−3.7	35.6
0431−360	DA10.0	10.8	−19.6	27.0	35.1
0431−279	DC9.5	11.5	−28.8	33.3	45.5
0433+270	DA9.3	−0.1	−19.8	7.0	21.1
0435−088	DQ8.0	−25.1	−63.2	−21.6	71.4
0457−004	DA4.7	−6.1	−23.8	2.5	24.7
0503−174	DAH9.5	32.2	42.5	41.0	67.2
0511+079	DA7.7	−14.5	−9.2	−30.6	35.1
0532+414	DA6.8	1.2	12.4	−13.4	18.2
0548−001	DQP8.3	4.6	6.3	10.5	13.1
0552−041	DZ11.8	−25.3	−65.7	−20.2	73.3
0553+053	DAP8.9	−12.2	−19.8	−31.2	38.9
0628−020	DA	−5.2	−7.7	−17.7	20.0
0615−591	DB3.2	−11.3	−0.1	7.1	13.3
0618+067	DA8.1	−9.0	−26.9	49.9	57.4
0620−402	DZ6	−13.9	−25.0	−7.2	29.5
0627+299	DA5	−0.80	−1.4	−0.6	1.7
0628−020	DA	61.0	−34.5	−27.2	75.2
0642−166	DA2	−0.6	−10.2	−14.5	17.7
0644+025	DA8	9.4	15.1	−30.9	35.7
0644+375	DA2.5	−19.7	−39.6	−32.7	55.1
0651−398A	DA7.0	5.2	28.7	8.9	30.5
0655−390	DA8.0	2.7	2.3	−28.2	28.4
0657+320	DC10.1	−31.7	−52.9	13.2	63.1
0659−063	DA7.8	−19.7	−37.5	−29.5	51.6
0708−670	DC	4.7	4.9	−19.9	21.1
0706+377	DQ7.6	−7.2	−13.0	−31.6	34.9
0727+482.1	DA10.0	−14.6	−40.5	−14.7	45.5
0727+482.2	DA10.0	−14.9	−41.1	−14.9	46.3
0728+642	DAP11.2	−4.5	−9.2	3.9	11.0
0736+053	DQZ6.5	0.6	−12.0	−18.4	21.9
0738−172	DAZ6.7	−30.5	−29.2	30.2	51.9
0743−336	DC10.6	49.4	67.6	61.4	103.9
0747+073.1	DA12.1	−76.7	−126.3	−49.0	155.7
0747+073.2	DA11.9	−76.7	−126.3	−49.0	155.7
0749+426	DC11.7	−17.8	−29.6	5.6	35.0
0751−252	DA10.0	19.1	15.5	−13.8	28.3
0752−676	DC10.3	−29.3	−15.4	13.6	35.9
0753+417	DA7.3	−13.8	−28.6	−3.5	31.9
0806−661	DQ4.2	−17.2	−6.5	7.3	19.8
0805+356	DA7.3	0.5	−4.9	−6.6	8.3
0810+489	DC6.9	−9.0	−15.1	5.0	18.3
0810+489	DC6.9	−14.5	−22.8	8.6	28.3
0816−310	DZ7.6	−45.0	−52.7	−37.0	78.6
0821−669	DA9.8	16.8	4.5	4.4	18.0
0827+328	DA6.9	4.1	−45.4	−6.6	46.1
0839−327	DA5.3	38.2	26.6	4.6	46.8
0840−136	DZ10.3	14.0	−0.0	−21.0	25.2
0843+358	DZ6	7.6	−5.5	−13.6	16.5
0856+331	DQ5.1	21.4	0.883	−24.3	32.4
0912+536	DCP7	21.0	−42.5	−24.3	53.3
0946+534	DQ6.2	20.2	−7.3	−16.1	26.9
0955+247	DA5.8	6.1	−28.1	−17.7	33.8
0955+247	DA5.8	19.1	−40.3	−11.8	46.2
0959+149	DC7	−39.4	56.1	−127.2	144.5
1009−184	DZ7.8	36.1	−8.8	−26.4	45.6
1009−184	DZ8.5	35.1	−6.0	−26.8	44.5
1012+083.1	DA7.8	38.4	10.1	−12.2	41.5
1019+637	DA7.3	−14.7	17.9	3.5	23.4
1033+714	DC9	138.8	−73.2	−58.0	167.3
1036−204	DQP10.2	36.0	17.9	20.7	45.2
1043−188	DQ8.1	110.7	−71.1	−107.8	170.1
1055−072	DA6.8	42.3	−10.4	−16.3	46.5
1105−048	DA3.5	−17.3	−37.8	−29.8	51.2
1116−470	DC	24.3	−9.2	−7.0	27.0
1121+216	DA6.7	57.8	−25.3	−21.5	66.7
1124+595	DA4.8	−12.2	1.3	6.0	13.7
1132−325	DC	−11.4	22.5	35.8	43.8
1134+300	DA2.5	9.2	−4.6	−2.9	10.7
1142−645	DQ6.4	−52.1	25.3	6.6	58.3
1149−272	DQ8.1	24.9	−8.5	−0.8	26.4
1202−232	DAZ5.8	3.0	6.1	8.6	11.0
1208+576	DAZ8.6	−45.5	−10.6	23.0	52.0
1214+032	DA8.0	64.0	−11.2	2.3	64.9
1223−659	DA6.5	0.7	0.1	−8.4	8.4
1236−495	DA4.4	24.0	−17.0	−8.6	30.7
1241−798	DC/DQ	38.1	−36.9	33.3	62.6
1242−105	DA6.3	13.8	−44.3	24.3	52.4
1257+037	DA8.7	−6.2	−69.4	−25.6	74.2
1309+853	DAP9	−16.3	−1.3	15.4	22.5
1310+583	DA4.8	−16.3	6.7	5.7	18.5
1310−472	DC11.9	−133.6	81.4	−51.5	164.8
1315−781	DA	−23.5	+26.4	−32.3	47.8
1315−781	DC8.8	−30.2	34.0	−41.7	61.7
1327−083	DA3.7	49.2	−76.6	−7.4	91.3
1334+039	DZ10.0	87.5	−122.2	8.5	150.5
1337+705	DAZ2.8	43.7	−15.5	29.9	55.1
1339−340	DA9.5	55.0	108.0	177.4	214.8
1344+572	DA3.8	27.3	26.8	37.5	53.5
1344+106	DAZ7.1	54.6	−62.3	14.1	84.1

Table 3
(Continued)

WD No.	Type	U	V	W	T
1345+238	DA10.7	67.0	−47.4	20.1	84.5
1350−090	DAP5	−21.7	−23.0	−23.2	39.2
1401+457	DC19	16.9	−27.6	5.5	32.9
1403+451	DB	3.9	−2.1	1.2	4.5
1425−811	DAV4.2	−7.9	−26.2	−44.0	51.779
1436−781	DA8.1	29.7	−32.5	23.3	49.8
1444−174	DC10.1	33.0	−61.4	17.6	71.9
1529+141	DA9.6	−10.6	−13.1	−7.2	18.3
1532+129	DA9.6	−1.8	−26.2	3.9	26.5
1538+333	DA5.6	12.0	−5.2	11.8	17.6
1544−377	DA4.7	5.5	−22.4	7.6	24.3
1609+135	DA5.8	−25.2	−35.3	−17.4	46.8
1620−391	DA2	−1.3	2.8	−3.2	4.5
1625+093	DA7.3	−23.9	−46.7	−12.3	53.9
1626+368	DZ5.5	35.1	15.5	35.6	52.3
1632+177	DA5	−2.7	2.3	−5.3	6.4
1633+433	DAZ7.7	−12.7	−4.2	−13.9	19.4
1633+572	DQ8.2	45.4	−3.0	54.5	71.0
1639+537	DAH6.7	−3.6	−19.1	8.9	21.4
1647+591	DAV4.2	−6.0	−3.0	−5.4	8.6
1655+215	DA5.4	−25.9	−35.9	−18.4	47.9
1655+215	DA5.4	−38.0	−39.0	−17.7	57.3
1658+440	DAP1.7	−6.6	33.0	28.2	43.9
1705+030	DZ7.1	−16.6	−23.1	−13.4	31.5
1729+371	DA7.3	−28.2	21.2	13.8	37.9
1748+708	DQP9.0	5.8	−10.8	34.2	36.3
1756+143	DA9.0	−36.3	−86.3	49.1	105.7
1756+827	DA7.1	8.8	−30.3	106.4	111.0
1814+134	DA9.5	−47.7	−72.0	−8.6	86.8
1817−598	DA5.8	−15.1	−22.9	2.3	27.6
1820+609	DA10.5	−9.8	−9.0	−19.7	23.7
1829+547	DQP7.5	2.8	−0.7	24.3	24.4
1840+042	DA5.8	32.0	−23.6	19.9	44.4
1900+705	DAP4.5	6.7	5.5	6.0	10.5
1917+386	DC7.9	−5.2	−5.7	−8.6	11.6
1917−077	DBQA5	−5.4	−6.4	−0.5	8.4
1919+145	DA3.5	−4.2	−5.0	−0.7	6.6
1935+276	DA4.5	16.0	10.2	−31.7	37.0
1953−011	DAP6.5	−32.3	−31.9	3.7	45.6
2002−110	DA10.5	40.4	9.8	−76.6	87.2
2007−303	DA3.3	−22.0	−18.3	18.0	33.8
2008−600	DC9.9	−17.7	−62.3	−3.3	64.9
2008−799	DA8.5	18.0	−6.5	−20.7	28.2
2011+065	DQ7	−64.2	−24.8	−17.0	70.9
2032+248	DA2.5	−36.9	−24.9	−2.8	44.7
2039−202	DA2.5	15.9	−3.9	−30.9	35.0
2040−392	DA4.5	−13.6	−25.2	−0.3	28.7
2039−682	DA3.1	0.698	−17.8	−9.9	20.4
2047+372	DA4	13.4	5.5	−1.4	14.6
2048+263	DA9.7	−37.6	−16.2	11.8	42.7
2048+263	DA9.7	−79.5	104.1	−13.4	131.7
2048−250	DA6.6	5.3	−13.6	−20.0	24.8
2054−050	DC10.9	31.1	−11.4	−54.1	63.5
2105−820	DAP4.9	12.5	−17.4	3.6	21.8
2117+539	DA3.5	−0.8	2.1	18.3	18.5
2115−560	DA6	17.5	−18.6	−31.4	40.5
2118−388	DC9.6	9.3	−6.3	−11.6	16.1
2126+734	DA3.8	3.2	11.8	−23.5	26.5
2133−135	DA5.0	11.7	−12.8	−20.3	26.7
2138−332	DZ7	−15.0	−8.3	8.4	19.1
2140+207	DQ6.1	−28.0	−18.9	−17.1	37.9
2149+021	DA2.8	−28.4	−3.2	−37.7	47.3
2151−015	DA6	−59.0	52.4	−85.8	116.6
2154−512	DQ7	−12.4	−22.4	9.9	27.5
2159−754	DA5	−27.6	7.6	18.5	34.1
2211−392	DA8	57.8	−43.7	−44.5	85.1

Table 3
(Continued)

WD No.	Type	U	V	W	T
2207+142	DA6.6	21.1	83.8	−45.7	97.7
2209−147	DA6.6	54.9	−21.5	30.4	66.3
2211−392	DA8.1	46.6	−43.1	−61.1	88.2
2215+386	DC10.6	48.7	−7.1	−20.6	53.3
2226−754	DC9.9	−0.5	−88.5	71.5	113.8
2226−755	DC12.1	−0.5	−88.5	71.5	113.8
2246+223	DA4.7	42.4	−10.4	−16.9	46.8
2248+293	DA9	111.2	−29.8	−43.0	122.9
2251−070	DZ13	68.0	−48.2	−50.0	97.2
2253+054	DA9	20.3	−33.8	−34.2	52.2
2311−068	DQ6.8	−45.3	−1.7	7.4	45.9
2322+137	DA10.7	3.2	−0.5	−0.3	3.2
2326+049	DAZ4.4	−31.6	−2.1	−1.3	31.7
2336−079	DAZ4.6	−5.8	−13.4	−5.9	15.8
2341+322	DA4.0	−18.8	5.6	−0.4	19.6
2347+292	DA9	−18.3	2.7	−57.2	60.1
2351−335	DA5.7	−62.0	−22.5	−38.2	76.2
2359−434	DAP5.8	13.9	−16.4	−27.6	35.0

Table 4
Kinematical Statistics of Spectroscopic Subgroups within 25 pc

Type	Number	$\langle U \rangle$	$\langle V \rangle$	$\langle W \rangle$	$\langle T \rangle$
DA/DAZ	133	2.5	−18.4	−5.8	48.9
		33.9	33.8	28.6	33.0
DQ	15	−2.4	−16.0	−3.3	46.8
		38.7	26.8	25.2	22.2
DZ	14	2.0	−21.5	−14.0	47.0
		35.0	20.4	25.3	25.0
DC	26	−4.1	−27.0	−7.8	66.6
		46.7	49.8	41.3	50.8
DAP/DAH	11	3.3	−10.2	0.9	42.0
		30.6	30.7	26.3	27.5
Mag.non-DA	5	4.2	−19.5	−0.4	47.0
		25.4	28.5	16.9	25.0

and careful consideration of this together with the use of individual galactic orbits (see Pauli et al. 2006 and others) may help to better separate these populations.

4. DQ STARS WITHIN 25 pc

In Figure 3, we display the distribution of $T_{\rm eff}$ for the 23 DQ WDs (upper panel) and 28 DC WDs (lower panel) within 25 pc. Although any comparison with the non-DA subgroups suffers from small number statistics, the number of DQ stars appears to peak at lower temperatures, as expected since the C_2 molecular absorption bands strengthen with decreasing $T_{\rm eff}$. Although the number of stars in both distributions is small, it is noteworthy that the DC stars extend to even lower temperatures than the DQ stars. The previously known precipitous cutoff in the number of DQ stars at surface temperatures cooler than ∼6500 is seen in Figure 3. This real cutoff was first noted by Bergeron et al. (2001) and subsequently found in the much larger Sloan Digital Sky Survey (SDSS) sample of DQ stars by Dufour et al. (2005) and by Koester & Knist (2006).

Returning to the temperature distribution of 28 DC stars and 23 DQ stars, while mindful of small number statistics, it is nonetheless interesting that we see a large increase in the number of DC stars beginning at or near the temperature at which the DQ cutoff is seen. While some of these DC stars may show line features at high enough spectral resolution and sensitivity while other DCs may turn out to be hydrogen-

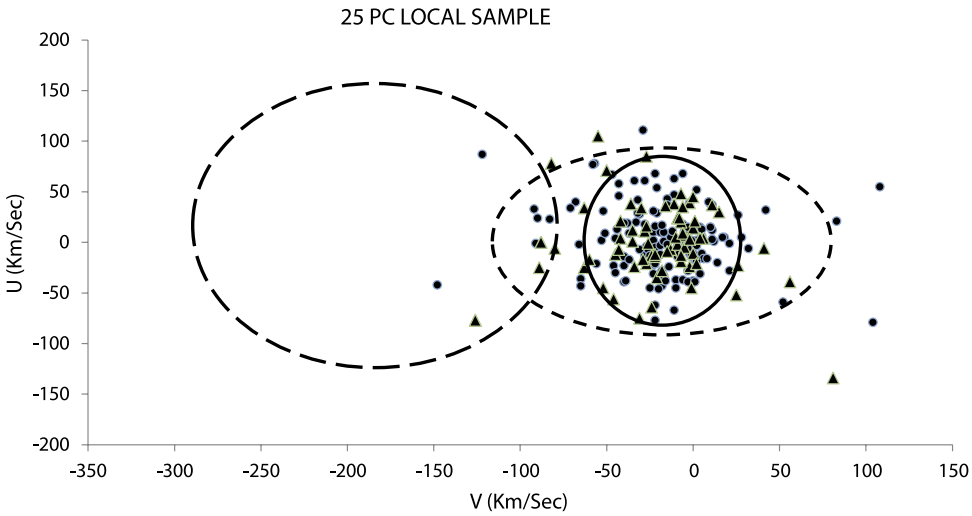

Figure 2. *U* vs. *V* space velocity diagram for the 25 pc sample of white dwarfs with the assumption of zero radial velocity. DA stars are denoted by closed circles, while non-DA stars are denoted by closed triangles. For comparison, three velocity ellipses for main sequence stars are shown following Chiba & Beers (2000): the 2σ velocity ellipse contour (solid line) of the thin disk component, the 2σ ellipse of the thick disk component (short-dashed line) and the 1σ contour of the halo component (long-dashed line).

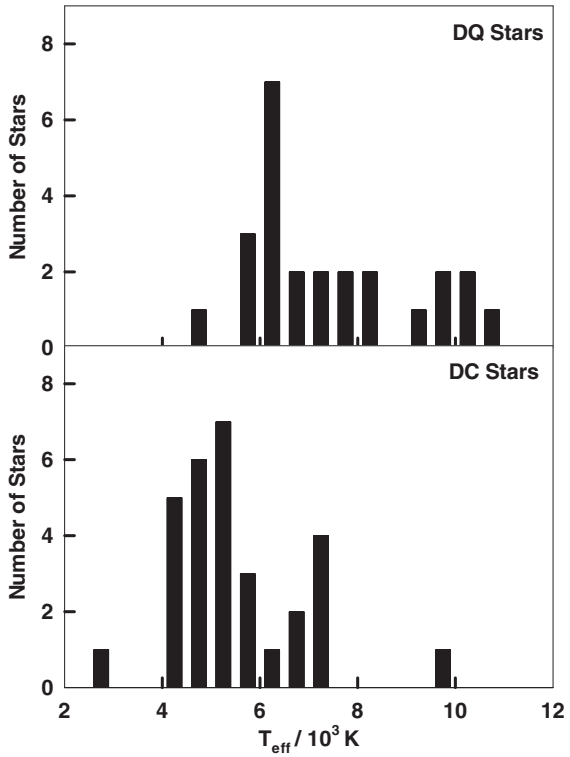

Figure 3. Histogram of the number vs. surface temperature distribution function for all DQ white dwarfs (upper panel) and all DC white dwarfs (lower panel) within 25 pc of the Sun. Note the pileup of DC stars near the temperature at which the DQ stars show a real cutoff.

dominated, we suggest the possibility that some of the 28 DCs within 25 pc could possibly be heretofore unidentified DQ stars with extreme pressure shifts that render their spectra unrecognizable. Alternatively, there may be some physical mechanism that removes carbon from the smallest optical depths in the atmosphere.

The peculiar DQ stars, the so-called C_2H stars, appear at the low temperature end of the DQ distribution of $T_{\rm eff}$. Hall & Maxwell (2008) pointed out that the peculiar absorption features first identified as C_2H in the spectra of cool ($T_{\rm eff} < 6000$ K) peculiar DQ stars were misidentified as hydrocarbon molecules, and instead are the extremely pressure-shifted Swan bands of C_2. Kowalski (2010) showed that the distortion of Swan bands originates in the pressure-induced increase in the electronic transition energy between states involved in the transition. Unfortunately, the predicted Swan band shifts are too large compared to the observed ones. Thus, the need for further work in this area is indicated.

5. MAGNETIC WHITE DWARFS WITHIN 25 pc

The true incidence of magnetic WDs in a volume-limited survey remains an open question. Out to 25 pc, we count a total of 19 magnetic degenerates, among which there are 14 DA magnetics and 5 non-DA magnetics. Liebert et al. (2003) presented evidence that the true incidence of detected magnetism among field WDs at the level of ~2 MG or greater, is at least 10%, and may be higher. The incidence of detected magnetism in our volume-limited sample is 8% but would be as high or higher than the Liebert et al. (2003) percentage if surveys of field strengths below 2 MG were carried out for our sample.

The relatively small number of magnetics within 25 pc prevents a determination of whether or not the field strength of a magnetic WD varies as a function of time (stellar age). For the same reason, we cannot say if the fraction of magnetic WDs is higher among cool star samples (e.g., samples of field WDs near the Sun) than among surveys of field WDs that extend out to greater volumes of space and hence sample hotter WDs. It remains an open question whether the number of magnetic WDs increases with decreasing $T_{\rm eff}$, luminosity, or cooling age. The answers to these questions must await volume-limited surveys sufficiently large in radius to encompass substantial numbers of hot WDs across a broader range of $T_{\rm eff}$.

6. COOL WHITE DWARFS WITH METALS

We count 26 cool WDs in the sample that exhibit absorption features due to accreted metals. This number excludes the DQ stars because although some may accrete metals, the carbon in their atmospheres is either primarily due to convective dredge-up (Dufour et al. 2005) or is primordial (Dufour et al. 2007). There has been no definitive explanation for why the DZ stars

and DQ stars appear to have mutually exclusive spectra; almost no DQ stars reveal absorption features due to metals (other than carbon), while the DZ stars rarely exhibit absorption features due to carbon. It is unlikely that accreted metals may be easier to hide in DQ atmospheres due to increased opacity provided by carbon. We note that Weidemann & Koester (1989) analyzed a DZ star that contained carbon. More recently, Koester et al. (2011) reported a DQ star from the SDSS that reveals a decrease in flux at the blue end, which could be explained with calcium and possibly iron. It is also possible that the apparent dichotomy between DQ and DZ stars could be due to selection and small number statistics. Moreover, since the DQ stars require very deep convection zones to dredge up carbon, it is also possible that any accreted metals are diluted to such an extent that metal features are too weak to be detected.

Among these 26 WDs within 25 pc are 2 DZAs, 13 DAZs, and 11 DZ stars. For these objects, the most likely source of the accreted metals is from debris disks (Farihi et al. 2009 and references therein).

On this basis, we speculate that all 26 non-DAs with photospheric metals accreted from dust/debris disks of tidally disrupted asteroids, or in the case of DAZ stars, from volatile-rich matter such as comets. Thus, we speculate that at least 11% of the WDs within 25 pc have circumstellar debris disks with rocky, metallic debris and very likely descended from main sequence progenitors that had planetary systems. By comparison with frequencies of occurrence of exoplanets among Sun-like stars, Howard (2013) and Mayor et al. (2011) find that 15% of Sun-like stars host one or more planets with mass $M\sin i$ = 3–30 Earth masses orbiting within 0.25 AU, and another 14% of Sun-like stars host planets with $M\sin i$ = 1–3 Earth masses. The similarity between the frequency of occurrence of exoplanets and the fraction of WDs with metal lines within 25 pc is almost certainly just a coincidence since we do not know exactly how many of the WDs in the 25 pc sample have been observed with high resolution.

Among the 25 pc sample in Table 1, we have uncovered three WDs with IR excesses from WISE photometry that were previously unknown. This is suggestive of debris disks (Cox et al. 2014) associated with the three WDs.

7. PRELIMINARY TESTS OF COOL WHITE DWARF SPECTRAL EVOLUTION

The total space density of WDs within 25 pc remains unchanged from the 20 pc sample (Holberg et al. 2008b), while the completeness drops from 85% at 20 pc to ~60% at 25 pc. The space density of WDs in Holberg et al. (2008b) is derived from the virtual completeness of the WDs within the core 13 pc sample. This can be determined in two ways: from a direct count of WDs within 13 pc, or by matching the slope of a log N – log (distance) plot to an expected slope of −3. The completeness estimates for the 20 pc and 25 pc samples are then simply computed with respect to the measured space density. Nevertheless, by considering the 20 pc sample, the nature of the incompleteness at 65% can be considered well characterized. We can use this knowledge to conduct a simple, preliminary, prospective test of WD spectral evolution to test the hypotheses that the ordinary DQ stars (i.e., excluding the class of hot DQs) are descendants of cooling DB stars (Koester et al. 1982; Wegner & Yackovich 1984).

The formation rate of DB stars can be estimated from the following expression:

$$\frac{dN}{dt} = f\frac{N_{\rm wd}}{t_{\rm DB}},$$

where f is the ratio of DB degenerates (Kleinman et al. 2004) to all other WD types within the observed range of $M_{\rm bol}$ for DB stars, $N_{\rm wd}$ is the local space density of WDs in the same range of $M_{\rm bol}$ as the DB stars, and $t_{\rm DB}$ is the time spent by DB stars cooling within their observed range of $M_{\rm bol}$. $N_{\rm wd}$ is obtained from a cool WD luminosity function.

The temperature range of the DB WDs is 30,000 K > $T_{\rm eff}$ > 12,000 K, corresponding to a luminosity range −1.01 > Log($L/L_{\odot}$) > −2.52. For DB stars, the local space density within the interval 12,000 K < $T_{\rm eff}$ < 30,000 K is

$$N_{\rm DB} \approx 2 \times 10^{-4}\ {\rm DBs\ pc^{-3}},$$

and the parameter f = 20% for DB stars (Kleinman et al. 2004). The 20 pc sample of Holberg et al. (2008) contained no spectroscopically identified DB stars. Bergeron et al. (2011) conducted a comprehensive analysis of 108 DB stars, including spectroscopic distance estimates, finding four DBs within 25 pc. One, WD2147+280, has a trigonometric parallax that yields a distance of 35.7 ± 0.4 pc, which, as the authors point out, is difficult to reconcile with the estimated distance unless the spectroscopic gravity is reduced to 8.2, in which case it becomes consistent with the larger distance. After calculating distance uncertainties from the results of Bergeron et al. (2011), we included three of these stars, WD1542−275, WD2058+392, and WD2316−173, in our new local sample including appropriate distance uncertainties. Overall, Bergeron et al. found a DB space density of 5.15×10^{-5} pc^{-3} that gives an expected number of approximately four DB WDs in the 25 pc sample, which compares favorably with the three DB stars included in our sample. If we assume an average DB mass, $M_{\rm DB} = 0.6\,M_{\odot}$, then the cooling timescale for a DB from 30,000 K to 12,000 K $t_{\rm DB} \approx 3.95 \times 10^{8}$ yr, according to the cooling models of Bergeron et al. (2011 and references therein).[4] Hence, the formation rate of DB stars, $dN_{\rm DB}/dt$, is

$$\frac{dN_{\rm DB}}{dt} = 1.01 \times 10^{-13}\ {\rm DB\ stars\ pc^{-3}\ yr^{-1}}.$$

Likewise for the formation rate of DQ stars from the following expression:

$$\frac{dN}{dt} = f\frac{N_{\rm wd}}{t_{\rm DQ}},$$

where f is the ratio of DQ degenerates to all other WD types within the observed range of $M_{\rm bol}$ for DQ stars, $N_{\rm wd}$ is the local space density of WDs in the same range of $M_{\rm bol}$ as the DQ stars, and $t_{\rm DQ}$ is the time spent by DQ stars cooling within their observed range of $M_{\rm bol}$. $N_{\rm wd}$ is obtained from a cool WD luminosity function.

The temperature range of the DQ stars is 12,000 K > $T_{\rm eff}$ > 5500 K, corresponding to a luminosity range of −2.52 > Log $L/L_{\odot}$ > −3.88. For the DQ stars, f = 9%. Assuming that DQ masses are $M_{\rm wd} = 0.6\,M_{\odot}$, the cooling time for a DQ through its interval of $M_{\rm bol}$ is $t_{\rm DQ} = 3.6 \times 10^{9}$ yr. The local space density of DQs within the interval 12,000 K > $T_{\rm eff}$ > 5500 K is $N_{\rm DQ} \approx 2 \times 10^{-3}$ DQs pc^{-3}. Thus, the formation rate of DQ stars, $dN_{\rm DQ}/dt$, is $dN_{\rm DQ}/dt = 4.5 \times 10^{-14}$ pc^{-3} yr^{-1}.

[4] http://www.astro.umontreal.ca/~bergeron/CoolingModels/

The lower formation for the DQ stars relative to DBs presumably may reflect that not all cooling DB stars become DQ stars and may become DA stars either through accretion of volatile-rich tidally disrupted bodies, interstellar H, or diffusive float up of H as the DB cools. This very tentative result must be confirmed with larger, more complete samples of WDs.

Although this evolution test is only preliminary (given the uncertainties in the parameters used), it is nonetheless illustrative of the far-reaching potential of enlarging the volume of space around the Sun containing known WDs, thus increasing the sample size of WDs in each astrophysically important spectroscopic subclass including the magnetic degenerates as well as the DA, DB, DQ, DZ, and DC degenerates.

8. CONCLUSIONS

Our study has revealed the distribution of WD spectral types for 224 degenerate stars in a volume-limited sample out to 25 pc. We find the following characteristics of the sample.

1. There is little or no evidence of halo or thick disk component members within 25 pc, but seven degenerates with extraordinarily high space motions.
2. The sample includes a sizable number of DQ stars and cool (mostly DC and DZ) WDs. We note a possibly significant pileup of DC stars at the low temperature cutoff of the DQ stars.
3. The incidence of magnetic WDs within 25 pc is 8% of the total sample. This is close to the estimate of the true incidence of field WDs in the galactic disk by Liebert et al. (2003).
4. We carry out a preliminary test of one scenario of WD spectral evolution theory, namely, that all of the DQ stars (excluding the "hot" DQs) are the evolutionary descendants of the DB WDs. Within the uncertainties in the true space densities of DB stars and DQ stars, we find preliminary evidence that the formation rate of DQ stars is smaller than the DB rate, suggesting that not all DB stars evolve into DQ stars below 12,000 K.
5. We find no compelling evidence of any significant differences between the space motions of the various spectroscopic subtypes.

As this study indicates that the local WD population, with its high degree of completeness, provides an invaluable ground truth sampling of the WD population, particularly in the galactic disk. As such, it affords a number of ways to help characterize much larger, deeper, and more distant WD samples that are not volume limited, for example, those from the SDSS. Toward that end, compelling motivation now exists to both increase the completeness of the current 25 pc sample and extend it to a greater distance, thus providing a larger basic sample. Such efforts will also set the stage for a time during the next decade when the European Space Agency *Gaia* mission will make possible a virtually complete determination of all WD distances and proper motions (but not necessarily stellar spectra) out to ~100 pc. Also within the same time frame, large surveys such as the Large Synoptic Survey Telescope will be sampling WD populations well into the halo.

This work is supported by NSF grant 1008845. We are grateful for several helpful comments and corrections from an anonymous referee. We thank John Debes for comments on the frequency of exoplanets around Sun-like stars. J.B.H. also wishes to acknowledge NASA Astrophysics Data Program grant NNX1OAD76. This research has made use of the White Dwarf Catalog maintained at Villanova University and the SIMBAD database, operated at CDS, Strasbourg, France.

REFERENCES

Bergeron, B., Wesemael, F., Dufour, P., et al. 2011, ApJ, 737, 28
Bergeron, P., Leggett, S., & Ruiz, M.-T. 2001, ApJS, 133, 413
Chiba, M., & Beers, T. 2000, AJ, 119, 2843
Cox, A., Sion, E., & Debes, J. 2014, BAAS, 223, 157.02
Dufour, P., Bergeron, P., & Fontaine, G. 2005, ApJ, 627, 404
Dufour, P., Bergeron, P., Liebert, J., et al. 2007, ApJ, 663, 1291
Farihi, J., Jura, M., & Zuckerman, B. 2009, ApJ, 694, 805
Giammichele, N., Bergeron, P., & Dufour, P. 2012, ApJS, 199, 29
Gianninas, A., Bergeron, P., & Ruiz, M.-T. 2011, ApJ, 743, 138
Gliese, W., & Jarheise, H. 1995, Catalog of Nearby Stars (version 3; Heidelberg: Astron. Rechen-Institut)
Greenstein, J. 1986, ApJ, 304, 334
Hall, P. B., & Maxwell, A. J. 2008, ApJ, 678, 1292
Holberg, J. B. 2008, JPhCS, 172, 1
Holberg, J. B., & Bergeron, P. 2006, AJ, 132, 1221
Holberg, J. B., Bergeron, P., & Gianninas, A. 2008a, AJ, 135, 1239
Holberg, J. B., Sion, E. M., Oswalt, T., et al. 2008b, AJ, 135, 1225 (LS08)
Howard, A. 2013, Sci, 340, 572
Kawka, A., & Vennes, S. 2006, ApJ, 643, 402
Kilic, M., Leggett, S. K., Tremblay, P.-E., et al. 2010, ApJS, 190, 77
Kleinman, S. J., Harris, H. C., Eisenstein, D. J., et al. 2004, ApJ, 607, 426
Koester, D., Girven, J., Gänsicke, B. T., & Dufour, P. 2011, A&A, 530, 114
Koester, D., & Knist, S. 2006, A&A, 454, 951
Koester, D., Weidemann, V., & Zeidler, E.-M. 1982, A&A, 116, 147
Kowalski, P. M. 2010, A&A, 519, L8
Liebert, J., Bergeron, P., & Holberg, J. B. 2003, AJ, 125, 348
Liebert, J., Dahn, C., & Monet, D. 1988, ApJ, 332, 891
Limoges, M.-M., Lepine, S., & Bergeron, P. 2013, AJ, 145, 136
Maxted, P., Marsh, T., & Moran, C. 2000, MNRAS, 319, 305
Mayor, M., Marmier, C., Lovis, S., et al. 2011, arXiv:1109.2497
McCook, G. P., & Sion, E. M. 1999, ApJS, 121, 1
Oswalt, T., Smith, J. A., Wood, M. A., & Hintzen, P. 1996, Natur, 382, 692
Pauli, E.-M., Napiwotzki, R., Altmann, M., et al. 2003, A&A, 400, 877
Pauli, E.-M., Napiwotzki, R., Heber, U., Altmann, M., & Odenkirchen, M. 2006, A&A, 447, 173
Sayres, C., Subasavage, J. P., Bergeron, P., et al. 2012, AJ, 143, 103
Silvestri, N., Oswalt, T. D., & Hawley, S. 2002, AJ, 124, 1118
Silvestri, N., Oswalt, T. D., Wood, M. A., et al. 2001, AJ, 121, 503
Sion, E. 1984, ApJ, 282, 612
Sion, E. M., Holberg, J. B., Oswalt, T. D., McCook, G. P., & Wasatonic, R. 2009, AJ, 138, 1681
Subasavage, J., Henry, T. J., Bergeron, P., et al. 2007, AJ, 134, 252
Subasavage, J. P., Henry, T. J., Bergeron, P., Dufour, P., & Hambly, N. C. 2008, AJ, 136, 899
Tremblay, P.-E., & Bergeron, P. 2008, ApJ, 672, 1144
Tremblay, P.-E., Bergeron, P., & Gianninas, A. 2011, ApJ, 730, 128
Wegner, G., & Yackovich, F. H. 1984, ApJ, 284, 257
Weidemann, V., & Koester, D. 1989, A&A, 210, 311
Wooley, R., Epps, E. A., Penston, M. J., & Pocock, S. B. 1970, ROAn, 5